

Type-II fractons from coupled spin chains and layers

Dominic J. Williamson¹ and Trithep Devakul²

¹*Stanford Institute for Theoretical Physics, Stanford University, Stanford, CA 94305, USA*

²*Department of Physics, Princeton University, NJ 08540, USA*

(Dated: December 9, 2021)

We describe a construction of topological orders from coupled lower dimensional symmetry-protected topological orders, which is closely related to gauging a subsystem symmetry. Our construction yields both conventional topological orders and exotic fracton topological orders of type-I and type-II. In particular, we find a coupled spin chain construction of Haah's cubic code, and a coupled layer construction of Yoshida's fractal spin liquids.

Fracton topological order is an exotic type of quantum order characterized by topological charges with restricted mobility due to superselection rules. To date, a wide range of 3D exactly solved models exhibiting fracton order have been discovered^{1–20}. The limited mobility of topological charges in these models has lead to topological quantum memories with unique advantages^{21–23}.

However, even the simplest class of fracton models, those described by commuting Pauli stabilizer Hamiltonians (see the appendix of Ref. 24 for a repository of models), require high degree interactions. This poses a significant barrier to any potential experimental realizations of fracton phases. To address this issue, several constructions of fracton models from coupled lower dimensional layers^{19,20,25–32} or spin chains^{33,34} have been found, some with much lower degree interactions.

In this work we introduce a construction of fracton stabilizer models²⁴ from coupled cluster state³⁵ layers, and spin chains, which are symmetry-protected topological (SPT) orders³⁶. In particular, we describe a construction of Haah's cubic code³⁷, the canonical type-II model, from coupled spin chains, featuring at most four body interactions. To the best of our knowledge³⁸ this is the first coupled spin chain construction of a model that has been rigorously shown to be type-II. We provide an explanation of how our coupled cluster state construction is related to the known construction of fracton models from gauging subsystem symmetries^{8,39–41}. We also describe a potential implementation of our construction by entangling spin systems, arranged in chains or layers, with some auxiliary quantum degrees of freedom that are then destructively measured.

We open in section I with several examples obtained via the general method explained in section II and III, then discussing an implementation of the construction in a modular architecture in section IV. Further examples are presented in appendix A.

I. EXAMPLES

Here we lead with some examples, as they can be presented before explaining the general construction. First we describe a coupled cluster chain construction of the 2D toric code⁴² and Haah's cubic code. We then de-

scribe a coupled cluster layer construction of Yoshida's type-II \mathbb{Z}_3 Fractal spin liquid (FSL), which generalizes to all FSL models⁵ (see the appendix). Further examples are worked through in the appendix. In the sections that follow we explain how these examples were found as instances of our general construction.

The examples in this paper make use of a description of Pauli stabilizer Hamiltonians in terms of a set of local generators $\{h_i\}_i$ for the stabilizer group $\langle\{h_i\}\rangle$. The commuting projector Hamiltonian whose ground space is the stabilizer codespace is given by the sum of generators

$$H = - \sum_i h_i. \quad (1)$$

The 2D toric code Hamiltonian⁴², governing qubits on the edges of a square lattice, is described by translates of the local stabilizer generators

$$\begin{array}{c} Z \\ | \\ Z \text{ --- } Z \end{array} , \quad \begin{array}{c} \text{--- } X \text{ --- } \\ | \quad | \\ X \text{ --- } X \end{array} , \quad (2)$$

where X, Z are Pauli matrices. This Hamiltonian can be constructed by coupling 1D cluster states³⁵ along the horizontal and vertical directions. The stabilizer generators for these decoupled cluster states are given by translates of

$$\begin{array}{c} | \\ Z - XI - Z \\ | \end{array} , \quad \begin{array}{c} Z \\ | \\ ZI - X - ZI \\ | \end{array} , \quad \begin{array}{c} Z \quad IZ \\ | \quad | \\ IX \text{ --- } \\ | \quad | \\ Z \quad IZ \end{array} , \quad (3)$$

where each vertex hosts two qubits, in addition to one on each edge. In the limit of a strong $-ZZ$ field on all vertices we recover the vertex-edge cluster state on the square lattice. Similarly in the limit of a strong $-(XX + ZZ)$ field on all vertices we find the 2D toric code Hamiltonian in Eq. (2) at leading order in perturbation theory.

Haah's cubic code is described by translates of the fol-

lowing local Hamiltonian terms, or stabilizer generators,

$$\begin{array}{c} IZ \text{ --- } ZI \\ | \qquad | \\ ZI \text{ --- } ZZ \\ | \qquad | \\ | \qquad | \\ II \text{ --- } IZ \\ | \qquad | \\ IZ \text{ --- } ZI \end{array} \quad , \quad
 \begin{array}{c} IX \text{ --- } XI \\ | \qquad | \\ XI \text{ --- } II \\ | \qquad | \\ | \qquad | \\ XX \text{ --- } IX \\ | \qquad | \\ IX \text{ --- } XI \end{array} \quad . \quad (3)$$

Surprisingly, we have found that this model can be obtained by coupling cluster chains stacked along three different directions. The Hamiltonians for these cluster chains are given by translates of the following local terms

$$\begin{array}{c} \text{ZIII} \\ | \\ \text{XIII} \\ | \\ \text{ZIII} \end{array} \quad , \quad
 \begin{array}{c} \text{ZIII} \\ | \\ \text{XIII} \\ | \\ \text{ZIII} \end{array} \quad , \quad
 \begin{array}{c} IZII \\ | \\ IXII \\ | \\ IZII \end{array} \quad , \quad
 \begin{array}{c} IZII \\ | \\ IXII \\ | \\ IZII \end{array} \quad , \quad
 \begin{array}{c} IIZI \\ | \\ IIXI \\ | \\ IIZI \end{array} \quad , \quad
 \begin{array}{c} IIZI \\ | \\ IIXI \\ | \\ IIZI \end{array} \quad , \quad
 \begin{array}{c} IIIZ \\ | \\ IIIX \\ | \\ IIIZ \end{array} \quad , \quad
 \begin{array}{c} IIIZ \\ | \\ IIIX \\ | \\ IIIZ \end{array} \quad ,$$

where each vertex and cube center now hosts four qubits, and the dotted lines indicate the dual lattice. In the limit of a strong $-(ZZII + IIZZ)$ field on the vertices and $-(ZZII + IIZI + IIZZ + XXXX)$ on the cube centers (dual vertices) we recover the cubic code Hamiltonian in Eq. (3) at leading order in perturbation theory.

The Hamiltonian for Yoshida's type-II \mathbb{Z}_3 FSL model

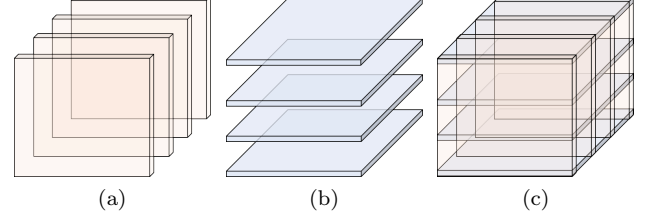


FIG. 1. (a) A stack of fractal cluster states in xy layers. (b) A stack of fractal cluster states in xz layers. (c) An FSL model obtained by coupling the xy and xz layers.

is a sum of translates of the following local generators

$$\begin{array}{c} IZ \text{ --- } IZ \\ | \qquad | \\ | \qquad | \\ ZZ \text{ --- } ZI \\ | \qquad | \\ ZI \text{ --- } ZI \end{array} \quad , \quad
 \begin{array}{c} IX^\dagger \text{ --- } IX^\dagger \\ | \qquad | \\ | \qquad | \\ XX^\dagger \text{ --- } XI \\ | \qquad | \\ XI \text{ --- } XI \end{array} \quad ,$$

where now X and Z are \mathbb{Z}_3 clock operators satisfying $XZ = e^{\frac{2\pi i}{3}} ZX$. We have found that this model can be obtained by coupling together fractal cluster state layers^{43–45} stacked along the \hat{y} and \hat{z} directions. The Hamiltonians for the fractal cluster state layers are given by translates of the following local generators

$$\begin{array}{c} IZ \text{ --- } IZ \\ | \qquad | \\ X \text{ --- } Z \\ | \qquad | \\ IZ \text{ --- } Z \end{array} \quad , \quad
 \begin{array}{c} \dots \dots \dots \dots \\ | \qquad | \qquad | \qquad | \\ \dots \dots \dots \dots \\ IX \text{ --- } Z \end{array} \quad ,$$

$$\begin{array}{c} ZI \text{ --- } ZI \\ | \qquad | \\ X \text{ --- } XI \\ | \qquad | \\ ZI \text{ --- } Z \end{array} \quad , \quad
 \begin{array}{c} \dots \dots \dots \dots \\ | \qquad | \qquad | \qquad | \\ \dots \dots \dots \dots \\ XI \text{ --- } Z \end{array} \quad .$$

where each vertex hosts two qubits, each xy or xz plaquette hosts a single qubit, and dotted lines again indicate the dual square lattice. If we group pairs of spins on xy and xz plaquettes onto the adjacent corner with minimal (x, y, z) coordinate, then in the limit of a strong $-(XX + ZZ^\dagger)$ field on these plaquette spins we find the FSL Hamiltonian in Eq. (4) at leading order.

We have found that the above coupled cluster state layer construction generalizes to all FSL models, see the appendix for further details. The general situation is depicted in Fig. 1, where the xy fractal cluster layers in Fig. 1a and xz fractal cluster layers in Fig. 1b are strongly coupled to produce the FSL model in Fig. 1c. In many cases (including the example above) the cluster layers can be further decomposed into coupled cluster chains.

II. GAUGING AND CLUSTER STATES

In this section we describe how certain cluster state models can be driven into topological phases by large on-site fields. In particular, we describe how to construct such a cluster state for any topological order that is obtained by gauging a subsystem symmetry following a generalized gauging procedure^{8,39–41}. Fig 2 shows this process applied to the 2D Ising model, resulting in the 2D toric code.

We define a *locally specified* symmetry to be a group whose elements are products of Pauli X matrices that commute with a set of local Pauli Z constraints. We utilize the stabilizer formalism⁴⁶ to describe these Pauli matrices via linear algebra over \mathbb{Z}_2 (\mathbb{Z}_d for qudits). In particular, a pair of basis vectors \hat{s}_X, \hat{s}_Z are assigned to every spin $s \in Q$ to keep track of the exponents of X_s and Z_s . Hence an arbitrary Pauli operator is described by

$$\prod_s X_s^{x(s)} Z_s^{z(s)} \mapsto \sum_s x(s) \hat{s}_X + z(s) \hat{s}_Z, \quad (5)$$

up to a \pm sign. The vector space describing all Pauli matrices P breaks up into a direct sum of subspaces describing products of X or Z matrices, $P = P_X \oplus P_Z$, respectively. We point out that $P_X \cong P_Z \cong \mathbb{Z}_2[Q]$.

We describe a set of Pauli Z constraint terms, Γ_c , indexed by $c \in C$ via a linear map $\sigma_Z : \mathbb{Z}_2[C] \rightarrow P_Z$ defined such that

$$\Gamma_c = \sigma_Z \hat{c}. \quad (6)$$

Here we focus on cases where the Γ_c are all local in two or three dimensional space. In the example, Fig. 2, σ_Z maps a bond c to the Ising ZZ interaction term across that bond. The violation, or excitation, of local constraints by Pauli X matrices is described by the map $\epsilon_Z : P_X \rightarrow \mathbb{Z}_2[C]$, where

$$\epsilon_Z = \sigma_Z^\dagger \Lambda, \quad (7)$$

with symplectic bilinear form $\Lambda : \hat{s}_X \leftrightarrow \hat{s}_Z$. This maps a Pauli X operator to the set of bond constraint terms it anticommutes with.

The constraints σ_Z determine a group of locally specified symmetries given by $\ker \epsilon_Z$. The locally specified symmetries can be further broken up into *local* and *global* symmetries by resolving as large a subspace of $\ker \epsilon_Z$ as possible via the image of a map $\sigma_X : \mathbb{Z}_2[G_{\text{loc}}] \rightarrow P_X$ that defines some local Pauli- X terms,

$$\Sigma_g = \sigma_X \hat{g}, \quad (8)$$

indexed by a set of generators $g \in G_{\text{loc}}$. The local symmetries are then given by $\text{im } \sigma_X \subseteq \ker \epsilon_Z$ and the global symmetries, modulo local symmetries, are given by $\ker \epsilon_Z / \text{im } \sigma_X$.

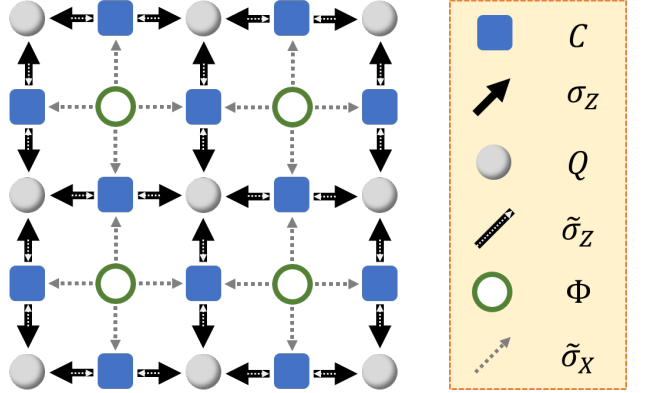


FIG. 2. The spins Q , constraints C , local relations Φ , and stabilizer maps $\sigma_Z, \tilde{\sigma}_Z, \tilde{\sigma}_X$, involved when gauging the 2D Ising model to obtain the 2D toric code.

Our starting point is a symmetric Hamiltonian in the paramagnetic phase

$$H = -\alpha \sum_s X_s - \sum_c \Gamma_c, \quad (9)$$

in the limit $\alpha \gg 1$. This model can be gauged following the general procedure introduced in Ref. 39 for gauging locally specified symmetries⁴⁷.

- The first step is to introduce a \mathbb{Z}_2 *gauge spin* c for each local constraint Γ_c . This extends the space of Pauli matrices to $P \oplus \tilde{P}$ where $\tilde{P} = \tilde{P}_X \oplus \tilde{P}_Z$ is the space of Pauli matrices on the gauge spins. We point out that $\tilde{P}_X \cong \tilde{P}_Z \cong \mathbb{Z}_2[C]$.
- Next we define gauge transformation operators $X_s A_s$, where $A_s = \tilde{\sigma}_Z \hat{s}$ for $\tilde{\sigma}_Z := \epsilon_Z$ considered as a map $\tilde{\sigma}_Z : \mathbb{Z}_2[Q] \rightarrow \tilde{P}_Z$ via the isomorphisms $\mathbb{Z}_2[Q] \cong P_X, \tilde{P}_Z \cong \mathbb{Z}_2[C]$, see Fig. 2. The original global symmetries can be recovered from products of the gauge transformation operators that act as identity on the gauge spins.
- Gauge invariant states, i.e. those with eigenvalue $+1$ under all gauge transformations, satisfy a generalized Gauss's law. A projection onto this gauge invariant subspace is then introduced. Here we only enforce such a projection energetically by adding terms to the Hamiltonian that introduce an energy penalty $\geq \Delta$ for violation of Gauss's law. In the limit of $\Delta \rightarrow \infty$ the projection becomes strict.
- Finally the other Hamiltonian terms are modified to include a minimal coupling to the gauge spins by projecting them onto the gauge invariant subspace. For our purposes this simply amounts to the change $\Gamma_c \mapsto X_c \Gamma_c$.

The gauged paramagnetic Hamiltonian is

$$H = -\alpha \sum_{s \in Q} X_s - \sum_{c \in C} X_c \Gamma_c - \Delta \sum_{s \in Q} X_s A_s. \quad (10)$$

This is a cluster Hamiltonian with a large X field applied to the s sites. See section III below for a further discussion of cluster states.

We consider the limit $\alpha \rightarrow \infty$ with Δ held constant. This effectively fixes out all the original Q spins in the $|+\rangle$ state. On the remaining C spins the Gauss's law terms become $X_s A_s \mapsto A_s$ and only products of minimally coupled constraint fields $X_c \Gamma_c$ that act trivially on the Q spins enter the effective Hamiltonian. These terms are all contained within $\ker \sigma_Z$, where we have made use of the isomorphism $\tilde{P}_X \cong \mathbb{Z}_2[C]$ to write $\sigma_Z : \tilde{P}_X \rightarrow P_Z$. In fact, all local terms in $\ker \sigma_Z$ appear at finite order in perturbation theory. Products of these terms are described by the image of a map $\tilde{\sigma}_X : \mathbb{Z}_2[\Phi] \rightarrow \tilde{P}_X$, satisfying $\text{im } \tilde{\sigma}_X \subseteq \ker \sigma_Z$, that resolves the maximal subspace of local terms in $\ker \sigma_Z$. In particular, only a set of local generators given by a choice of basis elements

$$B_\phi = \tilde{\sigma}_X \hat{\phi}, \quad (11)$$

for $\phi \in \Phi$, need to be included in the Hamiltonian. Other terms in $\text{im } \tilde{\sigma}_X$ are given by products of the generators B_ϕ , and their inclusion only results in a shifting of the energy levels without changing the quantum phase of matter. We remark that the B_ϕ terms were introduced by hand in the equivalent gauging construction of Ref. 39.

In the example in Fig. 2, gauge spins c live on the edges of the square lattice. The operators in $\text{im } \tilde{\sigma}_X$ are closed contractible loops of X operators, and B_ϕ is chosen to be the product of four gauge spins X_c around the plaquette ϕ . The effective Hamiltonian in the large α limit is simply the 2D toric code.

More generally, the effective Hamiltonian in the $\alpha \rightarrow \infty$ limit is given by

$$H = -\Delta \sum_s A_s - \sum_\phi B_\phi, \quad (12)$$

which corresponds to the CSS^{48,49} stabilizer map $\tilde{\sigma} = \tilde{\sigma}_X \oplus \tilde{\sigma}_Z : \mathbb{Z}_2[\Phi] \oplus \mathbb{Z}_2[Q] \rightarrow \tilde{P}$. The Hamiltonian in Eq. (12) is the same as the gauged and “disentangled” Hamiltonian from Ref. 39. Hence we have demonstrated that applying a large X field to the Q spins of the cluster Hamiltonian in Eq. (10) results in the model obtained by gauging the paramagnetic phase under the locally specified symmetry $\ker \sigma_Z$.

As an alternative to applying a large X field to the Q spins of the cluster Hamiltonian, we could instead measure them in the X basis. This procedure prepares the gauged model in some excited eigenstate. A correction operator can then be found to restore the model to its groundstate^{22,23}. See section IV for further discussion of this option.

III. COUPLING CLUSTER STATE LAYERS & CHAINS

In this section we describe a construction of certain cluster states by coupling together a number of different,

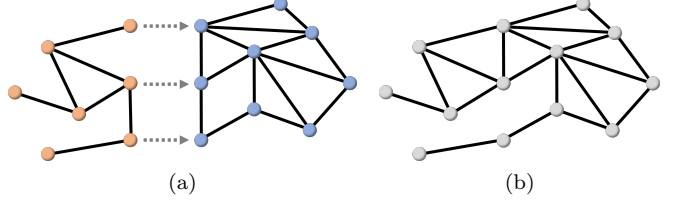


FIG. 3. (a) An example of graphs Θ (orange) and Θ' (blue) and a gluing map k (arrows) involving a subset of vertices. (b) The graph $\Theta \cup_k \Theta'$ obtained by gluing along k .

lower dimensional, cluster states. When combined with the results from the previous section this leads to a coupled cluster state layer construction for certain stabilizer topological orders.

A *cluster Hamiltonian* on an arbitrary graph Θ , with no self-loops or duplicate edges, is given by a sum of commuting Pauli terms

$$H_\Theta = - \sum_v X_v \prod_{v' \in N_v} Z_{v'}, \quad (13)$$

where v are vertices of the graph and N_v is the set of nearest-neighbor vertices connected by an edge to v . The cluster Hamiltonian is in the trivial phase if no symmetries are enforced. This follows from the local unitary equivalence

$$U H_\Theta U^\dagger = - \sum_v X_v, \quad \text{where } U = \prod_{\langle vv' \rangle} CZ_{vv'}, \quad (14)$$

where $\langle vv' \rangle$ denotes an edge in Θ between vertices v, v' , and CZ is a controlled- Z gate. This also reveals a simple construction of H_Θ ’s ground state $|\psi_0\rangle = U|+\rangle^{\otimes V}$ which is known as a *cluster state*. On the other hand, each cluster state respects a (potentially nontrivial) symmetry group determined by the graph Θ , which is given by Pauli- X operators that are products of the local terms in the Hamiltonian. The cluster state may lie in a nontrivial (subsystem) symmetry-protected topological phase^{36,43,50} with respect to this symmetry.

The Hamiltonian in Eq. (10) above is a cluster Hamiltonian on the *interaction graph* of the constraints σ_Z , under a large X field on s sites. The interaction graph of a set of constraints is a bipartite graph with a vertex for each spin and each constraint, with an edge connecting each constraint to the spins it acts nontrivially on.

To obtain a coupled layer construction for a gauged Hamiltonian, as in Eq. (10), we make use of an elementary *merging* and *splitting* property of cluster Hamiltonians. Essentially this boils down to the fact that two separate cluster Hamiltonians, one containing a vertex v and the other a v' , can be strongly coupled via a $Z_v Z_{v'}$ field to produce a single cluster Hamiltonian on a new graph where v and v' have been identified. More precisely, cluster Hamiltonians on the graphs Θ and Θ' can be coupled together to produce a model equivalent to a

cluster Hamiltonian on a new graph $\Theta \cup_k \Theta'$ in the strong coupling limit. Here k denotes an injective map from a subset λ of the vertices of Θ to the vertices of Θ' , see Fig. 3a. The graph $\Theta \cup_k \Theta'$ is obtained by *gluing* Θ to Θ' , i.e. identifying v with $k(v)$ for all $v \in \lambda$, see Fig. 3b. In the gluing process edges are added modulo 2, meaning that any doubled edges are deleted, i.e. if $\langle u, v \rangle \in \Theta$ and $\langle k(u), k(v) \rangle \in \Theta'$ then there is no $\langle u, v \rangle$ edge in $\Theta \cup_k \Theta'$, for any $u, v \in \lambda$.

The coupled Hamiltonian is given by

$$H(\alpha) = H_\Theta + H_{\Theta'} - \alpha \sum_{v \in \lambda} Z_v Z_{k(v)}. \quad (15)$$

In the $\alpha \rightarrow \infty$ limit the two qubit Hilbert space on vertices v and $k(v)$ is projected into the single qubit subspace with effective Pauli operators $X_v X_{k(v)} \mapsto \bar{X}_v$ and $Z_v \sim Z_{k(v)} \mapsto \bar{Z}_v$, where \sim indicates that these operators become identified within the subspace. Hence in the $\alpha \rightarrow \infty$ limit we have

$$\begin{aligned} H(\alpha) &= - \sum_{v \in \Theta \setminus \lambda} X_v \prod_{u \in N_v} Z_u - \sum_{v' \in \Theta' \setminus k(\lambda)} X_{v'} \prod_{u' \in N_{v'}} Z_{u'} \\ &\quad - \sum_{v \in \lambda} X_v X_{k(v)} \prod_{u \in N_v} Z_u \prod_{u' \in N_{k(v)}} Z_{u'} - \alpha \sum_{v \in \lambda} Z_v Z_{k(v)}, \\ &\mapsto H_{\Theta \cup_k \Theta'} \end{aligned} \quad (16)$$

at leading order in perturbation theory.

This implies that any cluster Hamiltonian H_Θ can be recovered by coupling together cluster Hamiltonians H_{θ_i} on a set of N subgraphs θ_i that cover Θ , with \mathbb{Z}_2 edge addition, i.e. $\Theta = \theta_1 \cup \theta_2 \cup \dots \cup \theta_N$. For appropriate graphs Θ this can result in a coupled layer or chain construction. For example the cluster state on the vertices and edges of a grid, see Fig. 4a, is given by coupled cluster chains, see Fig. 4b.

Combining the coupled cluster state construction from this section with the gauged paramagnet limit of a cluster Hamiltonian under a large X field in Eq. (10) yields a coupled cluster state construction of any gauged paramagnet Hamiltonian. The gauged Hamiltonian, Eq. (12), with interaction graph $\Theta = \cup_i \theta_i$ is obtained in the $\alpha \rightarrow \infty$ limit from

$$\sum_{i\text{-layer}} H_{\theta_i} - \alpha \sum_{v \in \Theta} \sum_{u \neq u' \in \Omega_v} Z_u Z_{u'} - \alpha \sum_{s \in Q} \prod_{u \in \Omega_s} X_u. \quad (17)$$

Where s runs over the Q vertices of Θ that are being projected out in Eq. (12) and Ω_v denotes the set of vertices in different subgraphs θ_i that become identified with v in Θ .

The largest degree interaction in the coupled cluster state Hamiltonian above is determined by the maximum degree of the cluster terms, which is one greater than the maximum degree of all the subgraphs θ_i , and the maximum degree of the $\prod X$ fields, which is the largest number of different subgraphs θ_i sharing a vertex that becomes identified with a Q vertex in Θ which gets

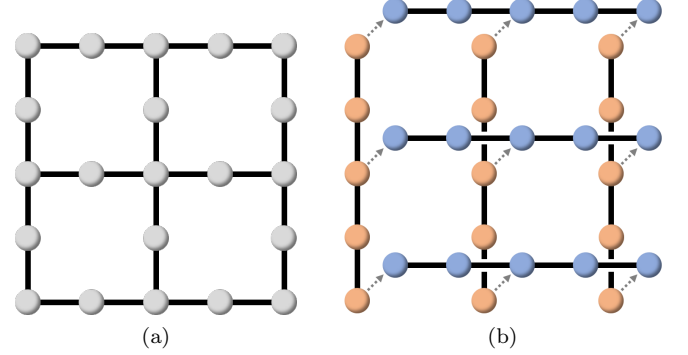


FIG. 4. (a) The cluster state corresponding to the gauged Ising model in Fig. 2. (b) A construction of (a) from coupled 1D cluster chains.

projected out. In particular, this leads to many coupled chain and coupled layer constructions of 2D and 3D topological stabilizer Hamiltonians with low interaction weight. This construction applies equally well to Hamiltonians with conventional topological order, type-I, and type-II fracton topological order, as demonstrated by the examples above and in the appendix.

IV. MODULAR ARCHITECTURE IMPLEMENTATION

In this section we describe an implementation of our coupled spin chain, and layer, constructions in modular architectures^{51–57} that combine static qubits arranged into 1D or 2D subsystems, such as ion traps or superconducting qubits, with auxiliary degrees of freedom that are not strictly constrained by locality, for example photonic qubits.

In the modular architecture the auxiliary qubits are those in $\{\Omega_s\}_{s \in Q}$ from Eq. (17), while the remaining qubits in each graph θ_i are stored in the static isolated subsystems with one or two dimensional locality. An additional auxiliary qubit, labelled by $\langle u, u' \rangle$, is introduced for each $Z_u Z_{u'}$ operator in Eq. (17) that is not contained within $\{\Omega_s\}_{s \in Q}$, to facilitate the measurement of this operator. The qubits in the static subsystems persist and hold the state of the desired stabilizer model, while the auxiliary qubits are entangled with the static subsystem qubits and then destructively measured to implement the desired stabilizer measurements on the static qubits.

The ground state of Eq. (12) is prepared by initializing all qubits in the $|+\rangle$ state and then entangling them via the CZ gates from Eq. (14) to create cluster states on the graphs θ_i . Next, a pair of CZ gates is applied to entangle each additional auxiliary qubit $\langle u, u' \rangle$, introduced above, with the qubits u and u' . The $Z_u Z_{u'}$ and $\prod X_u$ operators from Eq. (17) are then measured on the auxiliary qubits, projecting them into a unique state, decoupled from the static qubits. For the additional auxiliary qubits $\langle u, u' \rangle$,

this will involve a measurement in the X basis to implement the desired $Z_u Z_{u'}$ measurements on static qubits u and u' . If the stabilizer measurements all return the $+1$ eigenvalue, the desired ground state has been prepared. If any of the $Z_u Z_{u'}$ stabilizer measurements return -1 eigenvalues we can find a Pauli- X correction operator supported on the static qubits to flip these eigenvalues back to $+1$. If any of the $\prod_{u \in \Omega_s} X_u$ stabilizer measurements returns a -1 eigenvalue, we have effectively projected the static qubits into the -1 eigenvalue of the associated A_s operator. For topological codes⁵⁸, including fracton codes^{22,23}, we can decode these errors to find a Pauli- X correction operator. After applying the product of the correction operators, we have prepared a state within the desired ground space.

More generally, measurement of the A_s stabilizers on the static qubits can be performed following the above method. Measurement of the B_ϕ stabilizers can be accomplished similarly, by introducing a dual set of auxiliary qubits. Provided the rate of errors between measurement and correction steps is below the threshold for the code^{22,23,58} the measurement and correction process will successfully preserve logical information encoded into the ground space of the (fracton) topological code on the static qubits with high probability for sufficiently large system sizes. Hence for topological codes that admit a coupled layer construction, the procedure outlined in this section provides an implementation of topological error correction in a modular architecture, featuring low dimensional static subsystems coupled to long range auxiliary systems.

V. DISCUSSION & CONCLUSIONS

In this paper we have introduced coupled spin chain, and layer, constructions for topological stabilizer mod-

els, including conventional, type-I fracton, and type-II fracton topological orders. We based our construction on two key properties of cluster states. First, projecting out roughly half the spins with a large X field produces a gauged model on the remaining spins. Second, many cluster states naturally split into coupled lower dimensional cluster states. In particular, this provides a coupled cluster chain construction of Haah's cubic code and a coupled cluster layer construction of Yoshida's FSL models.

Our coupled layer constructions involve relatively low degree Hamiltonian interactions, thus paving the way towards experimental realization of exotic fracton topological orders. They are particularly well suited to modular architectures where qubits are organized into subsystems with inherent one or two dimensional local interactions. These subsystems need only interact with nonlocal auxiliary degrees of freedom that can be jointly measured for our scheme to be realizable.

Looking forward, it would be interesting to find a coupled layer construction of more general, possibly non-abelian, fracton models. We remark that our construction provides a hint in this direction, as the merging and splitting of cluster states also applies to generalized cluster states where the Z operators are replaced by other diagonal operators, such as \sqrt{Z} , CZ or multiply controlled- Z ^{59–61}. It would also be very interesting to derive topological defect networks from our coupled layer constructions.

ACKNOWLEDGMENTS

We acknowledge useful discussions with A. T. Schmitz. DW acknowledges support from the Simons foundation. TD acknowledges support from the Charlotte Elizabeth Procter Fellowship at Princeton University.

¹ C. Chamon, *Phys. Rev. Lett.* **94**, 40402 (2005), [arXiv:0404182](https://arxiv.org/abs/0404182) [cond-mat].

² J. Haah, *Phys. Rev. A - At. Mol. Opt. Phys.* **83**, 42330 (2011), [arXiv:1101.1962](https://arxiv.org/abs/1101.1962).

³ C. Castelnovo and C. Chamon, *Philos. Mag.* **92**, 304 (2012), [arXiv:1108.2051](https://arxiv.org/abs/1108.2051).

⁴ I. H. Kim, [arXiv](https://arxiv.org/abs/1202.0052) , 9 (2012), [arXiv:1202.0052](https://arxiv.org/abs/1202.0052).

⁵ B. Yoshida, *Phys. Rev. B - Condens. Matter Mater. Phys.* **88**, 125122 (2013), [arXiv:1302.6248](https://arxiv.org/abs/1302.6248).

⁶ J. Haah, *Phys. Rev. B - Condens. Matter Mater. Phys.* **89**, 75119 (2014), [arXiv:1310.4507](https://arxiv.org/abs/1310.4507).

⁷ S. Vijay, J. Haah, and L. Fu, *Phys. Rev. B - Condens. Matter Mater. Phys.* **92**, 235136 (2015), [arXiv:1505.02576](https://arxiv.org/abs/1505.02576).

⁸ S. Vijay, J. Haah, and L. Fu, *Phys. Rev. B* **94**, 235157 (2016), [arXiv:1603.04442](https://arxiv.org/abs/1603.04442).

⁹ S. Vijay and L. Fu, (2017), [arXiv:1706.07070](https://arxiv.org/abs/1706.07070).

¹⁰ A. Prem, S. J. Huang, H. Song, and M. Hermele, *Phys. Rev. X* **9** (2019), [10.1103/PhysRevX.9.021010](https://doi.org/10.1103/PhysRevX.9.021010), [arXiv:1806.04687](https://arxiv.org/abs/1806.04687).

¹¹ H. Song, A. Prem, S. J. Huang, and M. A. Martin-Delgado, *Phys. Rev. B* **99** (2019), [10.1103/PhysRevB.99.155118](https://doi.org/10.1103/PhysRevB.99.155118), [arXiv:1805.06899](https://arxiv.org/abs/1805.06899).

¹² A. Prem and D. Williamson, *SciPost Phys.* **7**, 068 (2019), [arXiv:1905.06309](https://arxiv.org/abs/1905.06309).

¹³ D. Bulmash and M. Barkeshli, *Phys. Rev. B* **100** (2019), [10.1103/PhysRevB.100.155146](https://doi.org/10.1103/PhysRevB.100.155146), [arXiv:1905.05771](https://arxiv.org/abs/1905.05771).

¹⁴ N. Tantivasadakarn and S. Vijay, (2019), [arXiv:1912.02826](https://arxiv.org/abs/1912.02826).

¹⁵ T. Devakul, W. Shirley, and J. Wang, *Phys. Rev. Res.* **2** (2020), [10.1103/physrevresearch.2.012059](https://doi.org/10.1103/physrevresearch.2.012059), [arXiv:1910.01630](https://arxiv.org/abs/1910.01630).

¹⁶ D. T. Stephen, J. Garre-Rubio, A. Dua, and D. J. Williamson, (2020), [arXiv:2004.04181](https://arxiv.org/abs/2004.04181).

¹⁷ N. Tantivasadakarn, (2020), [arXiv:2002.11345](https://arxiv.org/abs/2002.11345).

¹⁸ W. Shirley, (2020), [arXiv:2002.12026](https://arxiv.org/abs/2002.12026).

¹⁹ D. Aasen, D. Bulmash, A. Prem, K. Slagle, and D. J. Williamson, (2020), [arXiv:2002.05166](https://arxiv.org/abs/2002.05166).

²⁰ D. J. Williamson and M. Cheng, (2020), [arXiv:2004.07251](https://arxiv.org/abs/2004.07251).

²¹ S. Bravyi and J. Haah, *Phys. Rev. Lett.* **107**, 150504 (2011), arXiv:1105.4159.

²² S. Bravyi and J. Haah, *Phys. Rev. Lett.* **111**, 200501 (2013), arXiv:1112.3252.

²³ B. J. Brown and D. J. Williamson, *Phys. Rev. Res.* **2**, 1 (2020), arXiv:1901.08061.

²⁴ A. Dua, I. H. Kim, M. Cheng, and D. J. Williamson, *Phys. Rev. B* **100** (2019), 10.1103/PhysRevB.100.155137, arXiv:1908.08049.

²⁵ H. Ma, E. Lake, X. Chen, and M. Hermele, *Phys. Rev. B* **95**, 245126 (2017), arXiv:1701.00747.

²⁶ S. Vijay, (2017), arXiv:1701.00762.

²⁷ K. Slagle and Y. B. Kim, *Phys. Rev. B* **96**, 165106 (2017), arXiv:1704.03870.

²⁸ Y. Fuji, *Phys. Rev. B* **100** (2019), 10.1103/PhysRevB.100.235115, arXiv:1908.02257.

²⁹ A. T. Schmitz, S.-J. Huang, and A. Prem, (2019), arXiv:1901.10486.

³⁰ W. Shirley, K. Slagle, and X. Chen, (2019), arXiv:1907.09048.

³¹ X.-G. Wen, (2020), arXiv:2002.02433.

³² J. Wang, (2020), arXiv:2002.12932.

³³ G. B. Halász, T. H. Hsieh, and L. Balents, *Phys. Rev. Lett.* **119**, 257202 (2017), arXiv:1707.02308.

³⁴ T. H. Hsieh and G. B. Halász, *Phys. Rev. B* **96**, 165105 (2017), arXiv:1703.02973.

³⁵ H. J. Briegel and R. Raussendorf, *Phys. Rev. Lett.* **86**, 910 (2001), arXiv:0004051 [quant-ph].

³⁶ X. Chen, Z. C. Gu, Z. X. Liu, and X. G. Wen, *Science (80-.).* **338**, 1604 (2012), arXiv:1301.0861.

³⁷ J. Haah, *Commun. Math. Phys.* **342**, 771 (2016), arXiv:1407.2926.

³⁸ We were not able to find a proof that the “type-II” model in Ref. 34 supports no nontrivial string operators² and therefore satisfies the definition of type-II⁸.

³⁹ D. J. Williamson, *Phys. Rev. B* **94**, 155128 (2016), arXiv:1603.05182.

⁴⁰ W. Shirley, K. Slagle, and X. Chen, *SciPost Phys.* **6** (2019), 10.21468/scipostphys.6.4.041, arXiv:1806.08679.

⁴¹ A. Kubica and B. Yoshida, , 1 (2018), arXiv:1805.01836.

⁴² A. Y. Kitaev, *Ann. Phys. (N. Y.)* **303**, 2 (2003), arXiv:9707021 [quant-ph].

⁴³ T. Devakul, Y. You, F. J. Burnell, and S. Sondhi, *SciPost Phys.* **6** (2019), 10.21468/scipostphys.6.1.007, arXiv:1805.04097.

⁴⁴ T. Devakul and D. J. Williamson, *Phys. Rev. A* **98**, 022332 (2018), arXiv:1806.04663.

⁴⁵ T. Devakul, *Phys. Rev. B* **99** (2019), 10.1103/PhysRevB.99.235131, arXiv:1812.02721.

⁴⁶ D. Gottesman, (1997), arXiv:9705052 [quant-ph].

⁴⁷ Here we use a slightly different convention to Ref. 39, related by applying Hadamard gates to all gauge spins.

⁴⁸ A. R. Calderbank and P. W. Shor, *Phys. Rev. A - At. Mol. Opt. Phys.* **54**, 1098 (1996), arXiv:9512032 [quant-ph].

⁴⁹ A. Steane, *Proc. R. Soc. A Math. Phys. Eng. Sci.* **452**, 2551 (1996), arXiv:9601029 [quant-ph].

⁵⁰ Y. You, T. Devakul, F. J. Burnell, and S. L. Sondhi, *Phys. Rev. B* **98** (2018), 10.1103/PhysRevB.98.035112, arXiv:1803.02369.

⁵¹ D. D. Thaker, T. S. Metodi, and F. T. Chong, in *Lect. Notes Comput. Sci. (including Subser. Lect. Notes Artif. Intell. Lect. Notes Bioinformatics)*, Vol. 4297 LNCS (Springer, Berlin, Heidelberg, 2006) pp. 111–122.

⁵² L. Jiang, J. M. Taylor, A. S. Sørensen, and M. D. Lukin, *Phys. Rev. A - At. Mol. Opt. Phys.* **76** (2007), 10.1103/PhysRevA.76.062323, arXiv:0709.4539.

⁵³ D. L. Moehring, M. J. Madsen, K. C. Younge, R. N. Kohn, Jr., P. Maunz, L.-M. Duan, C. Monroe, and B. B. Blinov, *J. Opt. Soc. Am. B* **24**, 300 (2007).

⁵⁴ F. Helmer, M. Marzantoni, A. G. Fowler, J. Von Delft, E. Solano, and F. Marquardt, *Epl* **85** (2009), 10.1209/0295-5075/85/50007, arXiv:0706.3625.

⁵⁵ N. Y. Yao, L. Jiang, A. V. Gorshkov, P. C. Maurer, G. Giedke, J. I. Cirac, and M. D. Lukin, *Nat. Commun.* **3** (2010), 10.1038/ncomms1788, arXiv:1012.2864.

⁵⁶ K. Fujii, T. Yamamoto, M. Koashi, and N. Imoto, (2012), arXiv:1202.6588.

⁵⁷ C. Monroe, R. Raussendorf, A. Ruthven, K. R. Brown, P. Maunz, L. M. Duan, and J. Kim, *Phys. Rev. A - At. Mol. Opt. Phys.* **89** (2012), 10.1103/PhysRevA.89.022317, arXiv:1208.0391.

⁵⁸ E. Dennis, A. Kitaev, A. Landahl, and J. Preskill, *J. Math. Phys.* **43**, 4452 (2001), arXiv:0110143 [quant-ph].

⁵⁹ M. Levin and Z. C. Gu, *Phys. Rev. B - Condens. Matter Mater. Phys.* **86**, 115109 (2012), arXiv:1202.3120.

⁶⁰ X. Ni, O. Buerschaper, and M. V. den Nest, *J. Math. Phys.* **56** (2014), 10.1063/1.4920923, arXiv:1404.5327.

⁶¹ L. Fidkowski, J. Haah, M. B. Hastings, and N. Tantivasadakarn, (2019), arXiv:1906.04188.

⁶² J. Haah, , 200 (2013), arXiv:1305.6973.

⁶³ J. Haah, *Commun. Math. Phys.* **324**, 351 (2013), arXiv:1204.1063.

Appendix A: Further coupled layer examples

In this appendix we apply our coupled layer construction to a number of further examples including the 3D toric code⁵⁸, the X-cube model⁸, FSL models⁵, and cubic code B⁶.

1. 3D toric code

In this subsection we describe constructions of 3D toric code from 1D or 2D cluster states.

First we describe a construction of the 3D toric code from coupled 1D cluster states

$$\begin{array}{ccccccc}
 \begin{array}{c} \diagup \quad \diagdown \\ Z - X I I - Z \end{array} , &
 \begin{array}{c} \diagup \quad \diagdown \\ Z I I - X - Z I I \end{array} , &
 \begin{array}{c} Z \\ \diagup \quad \diagdown \\ - I X I - \end{array} , &
 \begin{array}{c} I Z I \\ X \\ \diagup \quad \diagdown \\ I Z I \end{array} , &
 \begin{array}{c} Z \\ \diagup \quad \diagdown \\ - I I X - \end{array} , &
 \begin{array}{c} I I Z \\ X \\ \diagup \quad \diagdown \\ I I Z \end{array} , & (A1)
 \end{array}$$

A strong $-(XXX + ZZI + ZIZ + IZZ)$ coupling on all vertices leads to

$$\begin{array}{ccccccc}
 \begin{array}{c} Z \quad Z \\ \diagup \quad \diagdown \\ Z - \quad Z \end{array} , &
 \begin{array}{c} \quad X \quad \\ X \quad X \\ \diagup \quad \diagdown \\ \quad X \quad \end{array} , &
 \begin{array}{c} X \quad X \\ \diagup \quad \diagdown \\ X \quad X \\ \diagup \quad \diagdown \\ \quad \quad \end{array} , &
 \begin{array}{c} \quad X \quad \\ X \quad X \\ \diagup \quad \diagdown \\ \quad X \quad \end{array} . & (A2)
 \end{array}$$

Further generalization to d -dimensional toric code from coupled 1D cluster states along d directions is clear.

The above construction of the d -dimensional toric code with qubits on edges from coupled 1D cluster states can be extended to a construction of the toric code with qubits on k -cells, for $1 < k < d$, from coupled k -dimensional cluster

states with qubits on $(k-1)$ - and k -cells. For example, 3D toric code from coupled 2D edge-face cluster states

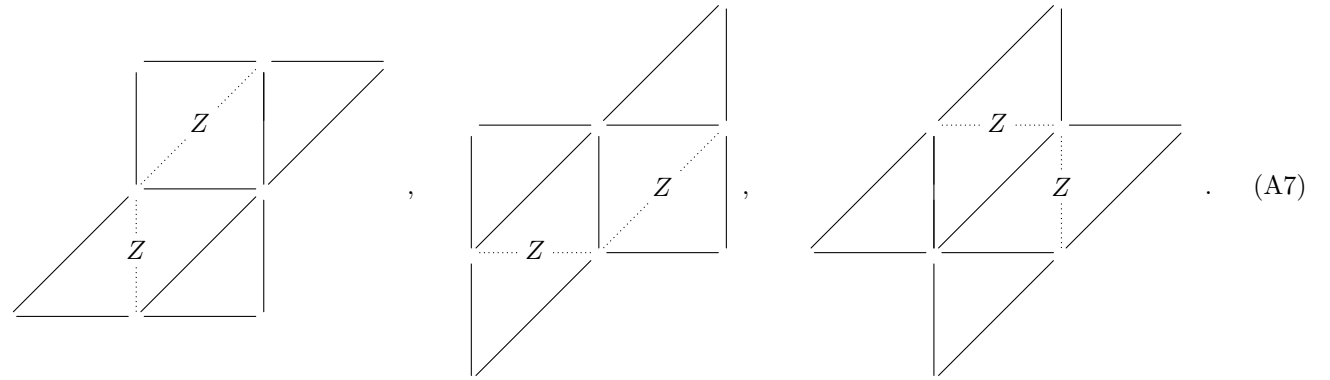
$$\begin{array}{c} \text{---} \quad \text{---} \\ | \quad \quad | \\ \text{---} \quad \text{---} \end{array} \quad , \quad
 \begin{array}{c} \text{---} \quad \text{---} \quad \text{---} \quad \text{---} \\ | \quad \quad | \quad \quad | \\ \text{---} \quad \text{---} \quad \text{---} \quad \text{---} \end{array} \quad , \quad
 \begin{array}{c} \text{---} \quad \text{---} \\ | \quad \quad | \\ \text{---} \quad \text{---} \\ \text{---} \quad \text{---} \\ | \quad \quad | \\ \text{---} \quad \text{---} \end{array} \quad , \quad (\text{A3})$$

$$\begin{array}{c} \text{---} \quad \text{---} \\ | \quad \quad | \\ \text{---} \quad \text{---} \\ \text{---} \quad \text{---} \\ | \quad \quad | \\ \text{---} \quad \text{---} \\ \text{---} \quad \text{---} \\ | \quad \quad | \\ \text{---} \quad \text{---} \end{array} \quad , \quad
 \begin{array}{c} \text{---} \quad \text{---} \\ | \quad \quad | \\ \text{---} \quad \text{---} \\ \text{---} \quad \text{---} \\ | \quad \quad | \\ \text{---} \quad \text{---} \\ \text{---} \quad \text{---} \\ | \quad \quad | \\ \text{---} \quad \text{---} \end{array} \quad , \quad
 \begin{array}{c} \text{---} \quad \text{---} \\ | \quad \quad | \\ \text{---} \quad \text{---} \\ \text{---} \quad \text{---} \\ | \quad \quad | \\ \text{---} \quad \text{---} \\ \text{---} \quad \text{---} \\ | \quad \quad | \\ \text{---} \quad \text{---} \end{array} \quad , \quad (\text{A4})$$

$$\begin{array}{c} \text{---} \quad \text{---} \\ | \quad \quad | \\ \text{---} \quad \text{---} \\ \text{---} \quad \text{---} \\ | \quad \quad | \\ \text{---} \quad \text{---} \\ \text{---} \quad \text{---} \\ | \quad \quad | \\ \text{---} \quad \text{---} \end{array} \quad , \quad
 \begin{array}{c} \text{---} \quad \text{---} \quad \text{---} \quad \text{---} \\ | \quad \quad | \quad \quad | \\ \text{---} \quad \text{---} \quad \text{---} \quad \text{---} \\ \text{---} \quad \text{---} \quad \text{---} \quad \text{---} \\ | \quad \quad | \quad \quad | \\ \text{---} \quad \text{---} \quad \text{---} \quad \text{---} \\ \text{---} \quad \text{---} \quad \text{---} \quad \text{---} \\ | \quad \quad | \quad \quad | \\ \text{---} \quad \text{---} \quad \text{---} \quad \text{---} \end{array} \quad , \quad
 \begin{array}{c} \text{---} \quad \text{---} \\ | \quad \quad | \\ \text{---} \quad \text{---} \\ \text{---} \quad \text{---} \\ | \quad \quad | \\ \text{---} \quad \text{---} \\ \text{---} \quad \text{---} \\ | \quad \quad | \\ \text{---} \quad \text{---} \end{array} \quad . \quad (\text{A5})$$

A strong $-(XX + ZZ)$ coupling on all edges leads to

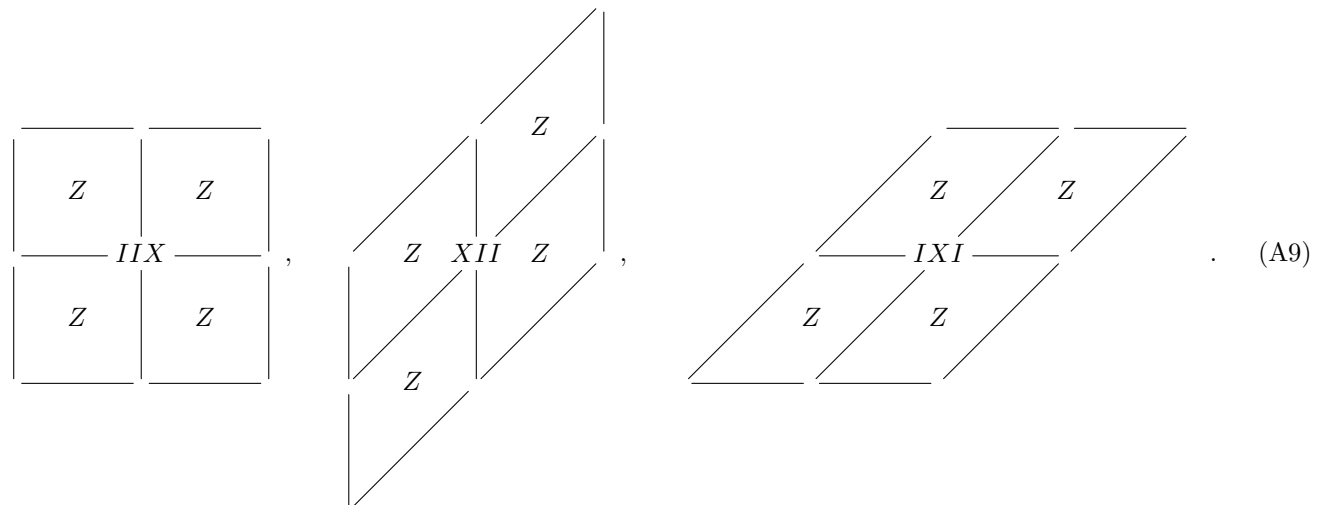
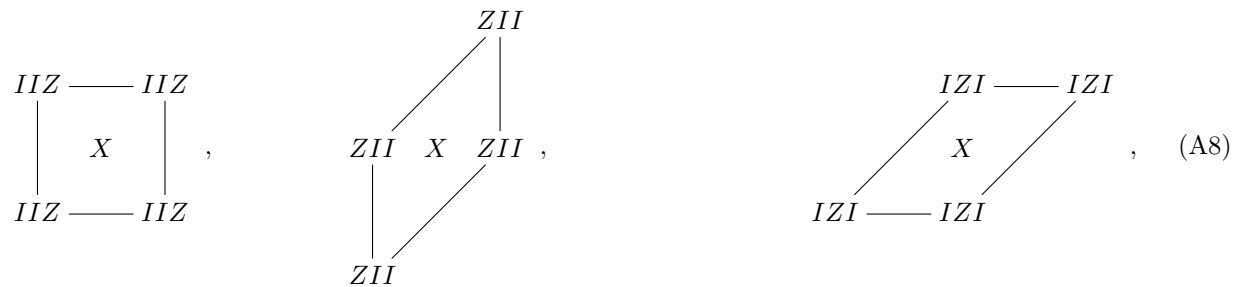
$$\begin{array}{c} \text{---} \quad \text{---} \\ | \quad \quad | \\ \text{---} \quad \text{---} \\ \text{---} \quad \text{---} \\ | \quad \quad | \\ \text{---} \quad \text{---} \\ \text{---} \quad \text{---} \\ | \quad \quad | \\ \text{---} \quad \text{---} \end{array} \quad , \quad (\text{A6})$$



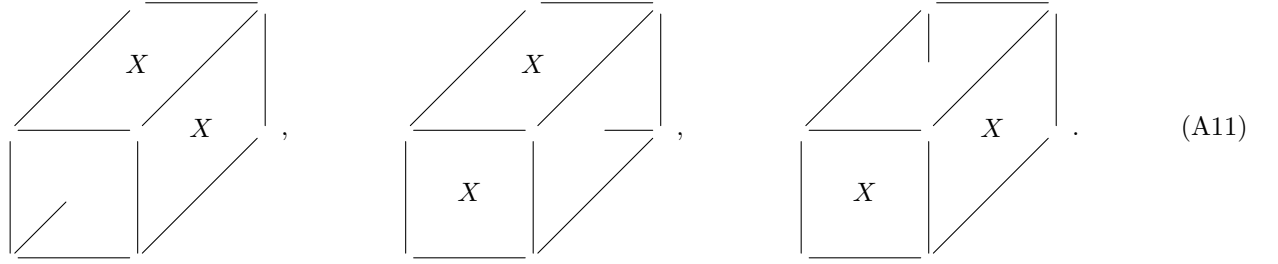
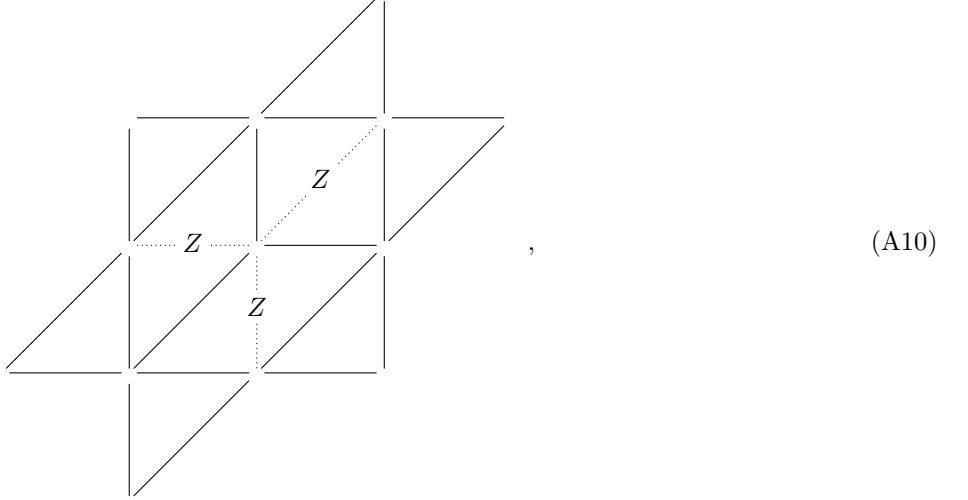
2. X-cube model

In this subsection we describe constructions of X-cube from coupled 2D or 1D cluster states.

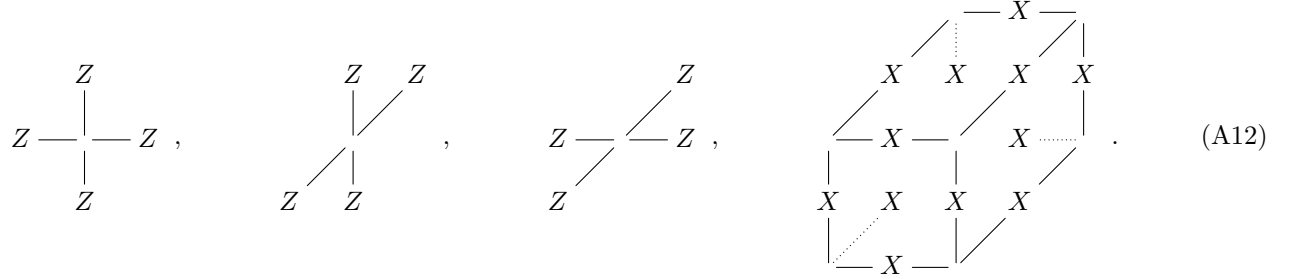
First we describe a construction from coupled 2D vertex-face cluster states



A strong $-(XX + ZZ)$ coupling on all edges leads to



Alternatively we also find a construction of X-cube from coupled 1D cluster states. Starting from Eq. (A1) and adding a strong $-(ZZZ + XXI + XIX + IXX)$ coupling to all vertices leads to



3. Fractal spin liquids

In this subsection we describe coupled 2D (and 1D) cluster state constructions of FSL models. We provide several examples: the Sierpinski type-I FSL, a type-II FSL, and cubic code written in FSL form. These are followed by a general construction for all FSL models.

First the Sierpinski FSL from coupled 2D fractal cluster states and 1D cluster states

$$(A13)$$

Grouping the z edge spins and xy plaquette spins onto the corner of minimal x, y, z , coordinate and adding a strong $-(XX + ZZ)$ coupling to these sites we find

$$(A14)$$

We can, in fact, further decompose the 2D fractal cluster states into coupled 1D cluster states

$$(A15)$$

which return the 2D fractal cluster states upon adding a strong $-IZZ$ coupling to the vertices and $-ZZ$ to the faces.

Next a type-II \mathbb{Z}_2 FSL

$$(A16)$$

$$(A17)$$

Grouping spins on xz and xy plaquettes to their minimal corner and adding a strong $-(XX + ZZ)$ coupling to these

sites,

$$\text{,} \quad \text{.} \quad (\text{A18})$$

The 2D fractal cluster states can be further broken up into coupled 1D cluster states

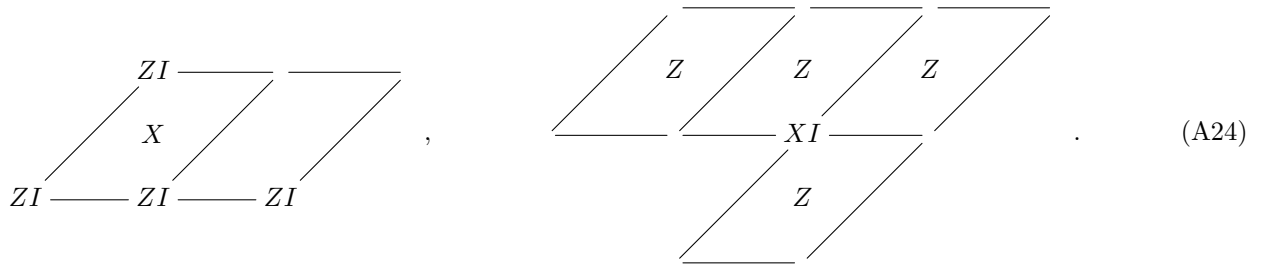
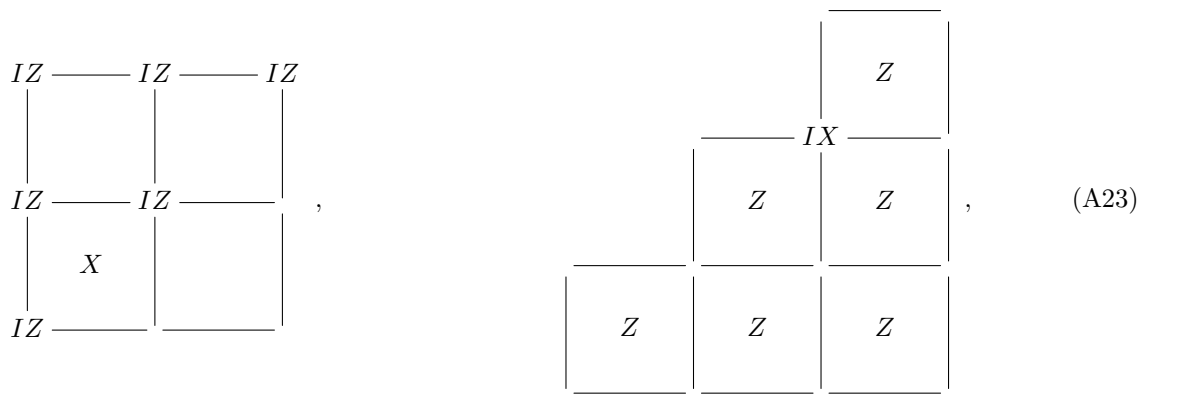
$$\text{,} \quad \text{.} \quad (\text{A19})$$

$$\text{,} \quad \text{.} \quad (\text{A20})$$

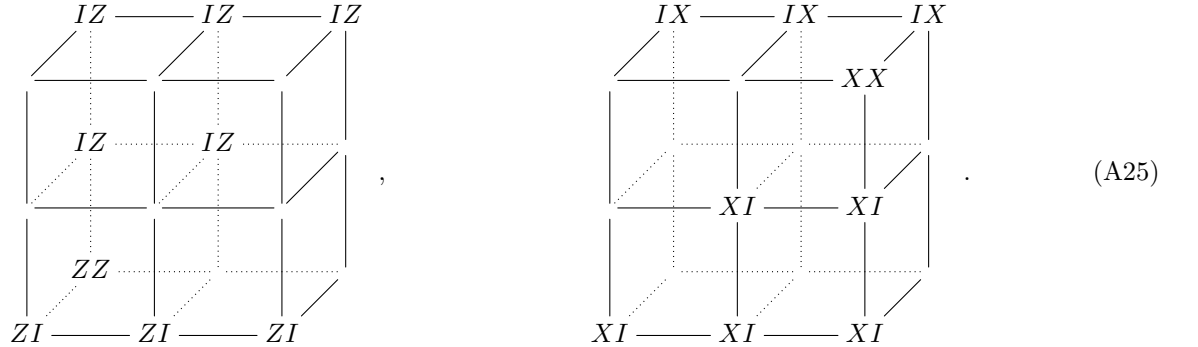
$$\text{,} \quad \text{.} \quad (\text{A21})$$

$$\text{,} \quad \text{.} \quad (\text{A22})$$

Now cubic code (written in FSL form) from coupled fractal cluster states



Grouping spins on xz and xy plaquettes to their minimal corner and adding a strong $-(XX + ZZ)$ coupling to these sites



a. General fractal spin liquids

Finally we describe a general coupled cluster layer construction for any FSL. The Hamiltonian, or stabilizer map, for any FSL can be written using the polynomial stabilizer formalism^{5,62,63}

$$\begin{pmatrix} 0 & G(\bar{x}, \bar{z}) \\ 0 & F(\bar{x}, \bar{y}) \\ F(x, y) & 0 \\ G(x, z) & 0 \end{pmatrix}, \quad (A26)$$

where $F(x, y) = 1 + f(x)y$, $G(x, z) = 1 + g(x)z$ for a first order FSL. For more general higher order FSL models we have

$$F(x, y) = 1 + \sum_{i \geq 1} f_i(x)y^i, \quad G(x, y) = 1 + \sum_{i \geq 1} g_i(x)z^i. \quad (A27)$$

We consider a stack of fractal cluster states along the \hat{y} and \hat{z} axes

$$\begin{pmatrix} 1 & 0 & 0 & 0 \\ 0 & 1 & 0 & 0 \\ 0 & 0 & 1 & 0 \\ 0 & 0 & 0 & 1 \\ 0 & F(\bar{x}, \bar{y}) & 0 & 0 \\ F(x, y) & 0 & 0 & 0 \\ 0 & 0 & 0 & G(\bar{x}, \bar{z}) \\ 0 & 0 & G(x, z) & 0 \end{pmatrix}. \quad (\text{A28})$$

We point out that the first and second qubits on every site are decoupled from the third and fourth. Hence the above Hamiltonian corresponds to a stack of decoupled layers.

Next we introduce strong on-site field couplings described by

$$\begin{pmatrix} 1 & 0 \\ 0 & 0 \\ 1 & 0 \\ 0 & 0 \\ 0 & 1 \\ 0 & 0 \\ 0 & 1 \\ 0 & 0 \end{pmatrix}. \quad (\text{A29})$$

To find the leading order Hamiltonian terms in perturbation theory we construct a minimal set of stabilizer generators that commute with the strong fields via linear combinations of columns from Eq. (A28)

$$\begin{pmatrix} 1 & 0 \\ 0 & G(\bar{x}, \bar{z}) \\ 1 & 0 \\ 0 & 0 \\ 0 & F(\bar{x}, \bar{y}) \\ 0 & F(\bar{x}, \bar{y})G(\bar{x}, \bar{z}) \\ F(x, y) & 0 \\ 0 & F(\bar{x}, \bar{y})G(\bar{x}, \bar{z}) \\ G(x, z) & 0 \end{pmatrix}. \quad (\text{A30})$$

Removing the first and third qubits from every site that are fixed out by the strong fields corresponds to dropping the odd numbered rows from the above matrix. This recovers the general FSL model in Eq. (A26).

The layered construction described here generalizes straightforwardly to FSL models involving more than two qubits per site. In fact it generalizes to any other model where the qubits can be partitioned into two disjoint subsets such that the Z stabilizer terms act on the first subset via functions of only (x, y) and on the second subset via functions of only (x, z) . For an example of this generalization see cubic code B below.

4. Cubic code B

In this subsection we describe a construction of cubic code B from coupled 2D fractal cluster states

$$\begin{array}{c} IIZZ \text{ ---} \\ | \\ IIIZ \text{ ---} IIZI \end{array} \quad , \quad \begin{array}{c} IIZI \text{ ---} \\ | \\ IIZZ \text{ ---} IIIZ \end{array} \quad , \quad \begin{array}{c} \overline{\text{---}} \quad \overline{\text{---}} \\ | \qquad | \\ ZI \qquad IZ \\ \overline{\text{---}} \quad \overline{\text{---}} \\ | \qquad | \\ IIXI \text{ ---} \\ | \\ \overline{\text{---}} \quad \overline{\text{---}} \\ | \qquad | \\ ZZ \end{array} \quad , \quad \begin{array}{c} \overline{\text{---}} \quad \overline{\text{---}} \\ | \qquad | \\ IZ \qquad ZZ \\ \overline{\text{---}} \quad \overline{\text{---}} \\ | \qquad | \\ IIIX \text{ ---} \\ | \\ \overline{\text{---}} \quad \overline{\text{---}} \\ | \qquad | \\ ZI \end{array} \quad , \quad (\text{A31})$$

$$\begin{array}{c}
 \text{IZII} \text{---} \text{ZZII} \\
 \diagup \quad \diagdown \\
 \text{XI} \\
 \diagup \quad \diagdown \\
 \text{ZIII} \text{---} \text{ZIII}
 \end{array} , \quad
 \begin{array}{c}
 \text{ZZII} \text{---} \text{ZIII} \\
 \diagup \quad \diagdown \\
 \text{IX} \\
 \diagup \quad \diagdown \\
 \text{IZII} \text{---} \text{ZIII}
 \end{array} , \quad (\text{A32})$$

$$\begin{array}{c}
 \text{ZI} \\
 \diagup \quad \diagdown \\
 \text{XIII} \text{---} \text{XIII} \\
 \diagup \quad \diagdown \\
 \text{ZZ} \text{---} \text{IZ}
 \end{array} , \quad
 \begin{array}{c}
 \text{IZ} \\
 \diagup \quad \diagdown \\
 \text{IXII} \text{---} \text{IXII} \\
 \diagup \quad \diagdown \\
 \text{ZI} \text{---} \text{ZZ}
 \end{array} . \quad (\text{A33})$$

Grouping the spins on xz and xy faces onto the corner of minimal x, y, z , coordinate and adding the strong $-(XIXI + IXIX + ZIZI + IZIZ)$ coupling to these sites we find

$$\begin{array}{c}
 \text{IIZZ} \text{---} \text{IIZZ} \\
 \diagup \quad \diagdown \\
 \text{IZIZ} \text{---} \text{ZZZI} \\
 \diagup \quad \diagdown \\
 \text{ZIII} \text{---} \text{ZIII}
 \end{array} , \quad
 \begin{array}{c}
 \text{IIZI} \text{---} \text{IIZI} \\
 \diagup \quad \diagdown \\
 \text{ZZZZ} \text{---} \text{ZIZZ} \\
 \diagup \quad \diagdown \\
 \text{IZII} \text{---} \text{IZII}
 \end{array} , \quad
 \begin{array}{c}
 \text{IIXI} \text{---} \text{IIXI} \\
 \diagup \quad \diagdown \\
 \text{IXIX} \text{---} \text{IXIX} \\
 \diagup \quad \diagdown \\
 \text{XIXX} \text{---} \text{XXII}
 \end{array} , \quad
 \begin{array}{c}
 \text{IIIX} \text{---} \text{IIIX} \\
 \diagup \quad \diagdown \\
 \text{IXXI} \text{---} \text{XXXX} \\
 \diagup \quad \diagdown \\
 \text{XIII} \text{---} \text{XIII}
 \end{array} , \quad (\text{A34})$$

the Hamiltonian for cubic code B (with a spatial rotation compared to Ref. 6).

Similar to the above examples, the 2D fractal cluster states can be further decomposed into coupled 1D cluster states.